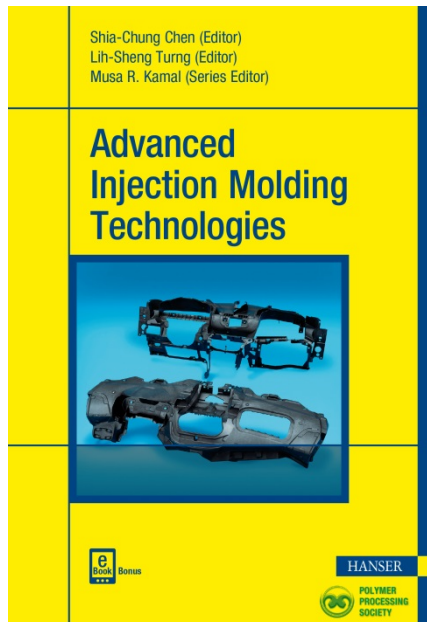


HANSER



Sample Pages

Advanced Injection Molding Technologies

Shiao-Chung Chen (Ed.) and
Lih-Sheng Turng (Ed.)

ISBN (Book): 9781569906033

ISBN (E-Book): 9781569906040

For further information and order see

www.hanserpublications.com (in the Americas)

www.hanser-fachbuch.de (outside the Americas)

© Carl Hanser Verlag, München

Contents

Preface	VII
1 Introduction to Injection Molding	1
<i>Shia-Chung Chen</i>	
1.1 Injection Molding and Molding Machines	1
1.1.1 Brief Overview of an Injection Molding Machine	3
1.1.2 Machine Setup for Process Conditions	4
1.1.2.1 Injection Pressure	4
1.1.2.2 Melt Temperature	5
1.1.2.3 Injection Speed	5
1.1.2.4 Mold Temperature	6
1.1.2.5 Other Parameters	7
1.2 Characterization of the Injection Molding Process	7
1.2.1 Injection Cycle	7
1.2.2 Mold Filling Stage	7
1.2.2.1 Process Overview	7
1.2.2.2 Flow Velocity and Melt Front Advancement	8
1.2.2.3 Pressure Variation and Distribution	9
1.2.2.4 Melt Temperature Variation and Distribution	10
1.2.2.5 Shear Stress and Shear Rate	12
1.2.3 Mold Packing/Holding Process	12
1.2.3.1 Process Overview	12
1.2.3.2 Packing Pressure Variation and Distribution	13
1.2.3.3 Packing Time	13
1.2.4 Mold Cooling Process	14
1.2.4.1 Process Overview	14
1.2.4.2 Coolant Temperature/Mold Temperature	14
1.2.4.3 Cooling Time/Ejection Temperature	15
1.2.4.4 Melt Temperature Distribution	15

1.3	Influence on Part Properties/Qualities	15
1.3.1	Effect of Processing Conditions on Part Properties	15
1.3.2	pvT Path and Thermal-Mechanical History	16
1.3.3	Shrinkage	17
1.3.4	Molecular Orientation/Fiber Orientation	17
1.3.5	Residual Stress	19
1.3.6	Warpage	21
1.3.7	Other Property/Quality Concerns	23
2	Intelligent Control of the Injection Molding Process	25
	<i>Yi Yang and Furong Gao</i>	
2.1	Introduction of Injection Molding Machine Control	25
2.2	Feedback Control Algorithms: Adaptive Control	27
2.2.1	Model Estimation	29
2.2.2	Model Predictive Control (MPC): Generalized Model Control (GPC)	30
2.2.2.1	Basic Principle of MPC and GPC	30
2.2.2.2	Parameter Tuning	33
2.2.2.3	Adaptive GPC Results	34
2.2.2.4	Adaptive GPC with Different Conditions	36
2.3	Fuzzy System in Injection Molding Control	37
2.3.1	Fuzzy Inference System Background	37
2.3.2	Fuzzy V/P Switchover	38
2.3.3	Fuzzy V/P System Experimental Test	43
2.3.4	Further Improvement	44
2.4	Learning Type Control for Injection Molding	48
2.4.1	Learning Type Control Background	48
2.4.2	PID-Type ILC	50
2.4.3	Time-Delay Consideration	51
2.4.4	P-Type ILC for Injection Velocity	52
2.4.5	P-Type ILC for Packing Pressure	54
2.5	Two-Dimensional Control Algorithm	55
2.5.1	Two-Dimensional Control Background	55
2.5.2	Two-Dimensional Dynamic Matrix Control	59
2.5.2.1	Problem Formulation	59
2.5.2.2	Controller Design	60
2.5.2.2.1	2D Equivalent Model with Repetitive Nature ..	60
2.5.2.2.2	2D Prediction Model	61
2.5.2.2.3	Cost Function and Control Law	62
2.5.2.2.4	2D-DMC Design Procedure	64
2.5.2.3	Analysis of Convergence and Robustness	65

2.5.3	Simulation Illustration	73
2.5.3.1	Case 1: Convergence Test	75
2.5.3.2	Case 2: Repetitive Disturbances	78
2.5.3.3	Case 3: Nonrepetitive Disturbances	80
2.5.4	Experimental Test of 2D-DMC	82
2.6	Summary and Perspectives	86
3	Water-Assisted Injection Molding	89
	<i>Shih-Jung Liu</i>	
3.1	Introduction	89
3.1.1	Molding Process	90
3.1.2	Advantages and Disadvantages	92
3.1.3	Water versus Gas	93
3.1.4	Molding Resins	94
3.2	Tooling	95
3.3	Process Parameters	97
3.3.1	Water Penetration Behavior in Molded Parts	97
3.3.2	Water Channel Geometry	99
3.3.3	Part Fingering	100
3.3.4	Unstable Water Penetrations	102
3.3.5	Molding of Fiber-Reinforced Materials	103
3.4	Morphology Development	105
3.5	Modeling and Simulation	108
3.6	Conclusions	112
4	Foam Injection Molding of Conductive-Filler/ Polymer Composites	115
	<i>Amir Ameli and Chul B. Park</i>	
4.1	Introduction	115
4.2	Conductive-Filler/Polymer Composites (CPCs)	116
4.3	Foam Injection Molding	119
4.4	Foam-Injection-Molded CPCs	120
4.4.1	Microstructure of CPC Foams	122
4.4.1.1	Fiber Interconnectivity	123
4.4.1.2	Fiber Orientation	124
4.4.1.3	Skin Layer	126
4.4.1.4	Fiber Breakage	127
4.4.2	Conductivity of CPC Foams	129
4.4.2.1	Through-Plane Conductivity	129

4.4.2.2 In-Plane Conductivity and Anisotropy	133
4.4.2.3 Uniformity of Conductivity	135
4.4.3 Impact of Processing Conditions on the Conductivity of CPC Foams	136
4.4.3.1 Degree of Foaming	136
4.4.3.2 Injection Flow Rate	142
4.4.3.3 Gas Content	144
4.4.3.4 Melt Temperature	145
4.5 Concluding Remarks	146
5 Water-Assisted Foaming: A New Improved Approach in Injection Molding	149
<i>Rachmat Mulyana, Jose M. Castro, and L. James Lee</i>	
5.1 Introduction	149
5.2 Need for Water-Carrier Particles	151
5.2.1 Evaluation of Water-Carrier Particles	151
5.2.2 Pressurized Water inside the Pellet	156
5.2.3 Residual Water and Drying after Molding	157
5.2.4 Shell Life of Pressurized Pellets	158
5.3 Injection-Molding Analysis	162
5.3.1 Molds and Molding Parameters	162
5.3.2 Experimental Observations during the Filling Stage	163
5.3.3 Packing and Cooling Stage	166
5.4 Mechanical Properties	170
5.4.1 Mechanical Property Comparison at Minimum Cycle Time	170
5.4.2 Effect of Packing Time on Mechanical Properties	171
5.4.3 Effect of Water Level on Mechanical Properties	172
5.5 Warping and Surface Quality	173
5.5.1 Warpage Improvement	173
5.5.2 Flow Marks and Surface Quality	175
5.5.3 Hiding the Flow Marks Using In-Mold Coating	177
5.5.4 Method of Weight Saving	178
5.6 Accelerated-Aging Test	182
5.6.1 Effect of Water-Carrier Particles	182
5.6.2 Effect of Residual Water	183
5.7 Comparison with Supercritical Fluid Molding (SCF Molding)	184
5.7.1 Experimental Setup	185
5.7.2 Mechanical Property Comparison	188
5.7.3 Warpage and Surface Quality	189
5.8 Summary and Conclusion	191

6	Variable Mold Temperature Technologies	195
<i>Shia-Chung Chen</i>		
6.1	Introduction	195
6.2	Various Methods for Dynamic Mold Temperature Control	197
6.3	Variable Mold Temperature Control with Embedded Internal Heat Sources	199
6.3.1	Hot Water Heating/Cold Water Cooling	199
6.3.2	Oil Heating/Water Cooling	199
6.3.3	Steam Heating/Water Cooling (RHCM)	200
6.3.4	Electrical Heater Heating	203
6.3.5	Pulse Cooling (Alternating Temperature Technology)	204
6.3.6	Electrical Heating at the Mold Surface Using a Two-Layer Coating	205
6.4	Mold Heating Based on Electromagnetic Induction Technology	206
6.4.1	Principle and Characteristics of Induction Heating	206
6.4.2	Induction Heating from Mold Surface (External Heating)	208
6.4.3	Induction Coil Design for Mold and Molding	209
6.4.4	The Challenges Facing EIHTC Applications and Their Possible Solutions	212
6.4.5	The Real Application of EIHTC – Mold Exterior Induction Heating	215
6.4.5.1	Elimination of a Weld Line and Floating Fiber Marks	215
6.4.5.2	Micro-Features Molding	216
6.4.6	Mold Exterior/Induction Heating by an Externally Wrapped Coil	217
6.4.7	Induction Heating from the Mold Interior Using Embedded Coils	220
6.4.8	Mold Interior/Proximity Effect Induced by Internal Current	224
6.5	Other Mold Surface Heating Technologies	227
6.5.1	Hot Gas-Assisted Heating	227
6.5.2	Infrared Heating	231
7	CAE for Advanced Injection Molding Technologies	235
<i>Rong-Yeu Chang and Chao-Tsai (CT) Huang</i>		
7.1	Introduction	235
7.2	Multi-Component Molding	236
7.2.1	Introduction	236
7.2.2	Governing Equations	238
7.2.3	Case Study	240
7.2.4	Summary	248

7.3	Long-Fiber Microstructure Prediction	249
7.3.1	Introduction	249
7.3.2	Governing Equations	250
7.3.3	Case Study	252
7.3.4	Summary	256
7.4	Microcellular Injection Molding	256
7.4.1	Introduction	256
7.4.2	Governing Equations	257
7.4.3	Case Study	259
7.4.4	Summary	264
7.5	Gas-Assisted Injection Molding	265
7.5.1	Introduction	265
7.5.2	Governing Equations	266
7.5.3	Case Study	267
7.5.4	Summary	271
7.6	Advanced Hot Runner	271
7.6.1	Introduction	271
7.6.2	Governing Equations	272
7.6.3	Case Study	273
7.6.4	Summary	281
7.7	Conformal Cooling System	281
7.7.1	Introduction	281
7.7.2	Governing Equations	282
7.7.3	Case Study	282
7.7.4	Summary	289
7.8	Variotherm Molding Technologies	289
7.8.1	Introduction	289
7.8.2	Governing Equations	290
7.8.3	Case Study	290
7.8.4	Summary	300
7.9	Injection–Compression Molding	301
7.9.1	Introduction	301
7.9.2	Governing Equations	302
7.9.3	Case Study	302
7.9.4	Summary	313
7.10	Concluding Remarks	313
8	Injection Molding of Optical Products	317
	<i>Pei-Jen Wang</i>	
8.1	Introduction	317

8.2 Optical Qualities	318
8.3 Design Guidelines	321
8.4 Fundamentals of Optics	322
8.4.1 Snell's Law and Lens Images	323
8.4.2 Monochromatic Aberrations	324
8.4.3 Zernike Polynomials	327
8.4.4 Abbe Number	328
8.5 Material Properties	329
8.6 Mold Flow Analysis	331
8.7 Case Studies	338
8.7.1 The Lens and the Mold	338
8.7.2 CAE Simulation Process	339
8.7.3 Experimental Verification	343
8.8 Concluding Remarks	347
9 Microinjection Molding	349
<i>Eusebio Cabrera, Jose M. Castro, Allen Y. Yi, and L. James Lee</i>	
9.1 Introduction	349
9.2 Issues in Molding Parts with Microfeatures	350
9.3 Influencing Factors in Microinjection Molding	354
9.4 Experimental and Numerical Studies of Injection Molding with Microfeatures	355
9.5 Developments in Microinjection-Molding Technology	363
9.6 Ultrathin Wall Case Study	368
9.7 Concluding Remarks	375
10 Mold Design/Manufacturing Navigation System with Knowledge Management	379
<i>Wen-Ren Jong</i>	
10.1 Introduction	379
10.2 Knowledge Management	381
10.3 Four-Layer Architecture	393
10.4 Redevelopment	402
10.5 Stage Integration	410
10.6 Conclusions	417
Index	419

Preface

Injection molding is arguably one of the most important polymer processing methods, accounting for approximately one-third of thermoplastics processed, and has been ranked No. 1 in terms of total product value, number of machines built and sold, and overall number of jobs. Many injection molding-related books published in the past have extensively covered the core topics of injection molding, such as material selection, process optimization, part and mold designs, tooling, special injection molding processes, and computer modeling and simulation, just to name a few.

However, since the beginning of the 21st century, due to growing environmental concerns, green molding and lightweight molding have received a lot of attention from the injection molding industry. As a result, novel engineering advancements (technology push) and increasing customer and societal demands (technology pull) have dramatically changed the technological landscape of this important process. Driven by calls to minimize the environmental footprint and save energy, the injection molding industry has witnessed the widening adoption of intelligent control and the growing applications of microinjection molding, microcellular injection molding, water-assisted foaming, and water-assisted injection molding, as well as variable mold temperature technologies. It has also seen emerging applications of conductive polymers and injection-molded optical plastic components. As special injection molding processes are being adopted, modeling and simulation of those novel processes have also been developed and become commercially available to aid with design, processing, and optimization. Finally, as the time-to-market continues to be compressed and knowledge management becomes one of the most important corporate assets, an automated mold design navigation system is expected to become a common tool for the injection molding industry. Given all of these changes, this book strives to educate current and future generations of scientists and engineers on the latest injection molding techniques and processes, which have not been comprehensively covered in any other textbooks to date.

Under the encouragement of the Taiwanese Ministry of Education (MOE) Man-power Cultivation Program for Advanced Manufacturing, many members of the

Society of Advanced Molding Technologies (SAMT), and Professor Musa Kamal, Series Editor of the Polymer Processing Society (PPS) book series Progress in Polymer Processing (PPP), we decided to take on this initiative and work with experts in the field to develop a new textbook that incorporates and covers industry-relevant topics so that it can meet the training requirements of the injection-molding industry.

We are truly grateful to the many chapter authors for their efforts and contributions. We are also deeply indebted to staff members at Carl Hanser Verlag GmbH & Co. KG; in particular, Mark Smith, Julia Diaz Luque, and Cheryl Hamilton for their technical assistance in every stage of this book development project. We are also grateful for our colleagues; especially Mrs. Jane Lai and Ms. Chris Lacey, for their administrative and editorial assistance. Finally, we hope that this book will bring useful information to readers like you and your organizations, and we look forward to hearing your constructive criticisms and suggestions, so that we will be able to improve its content in future editions.

Shia-Chung Chen and Lih-Sheng (Tom) Turng

Introduction to Injection Molding

Shia-Chung Chen

■ 1.1 Injection Molding and Molding Machines

Injection molding is an important thermoplastic processing technique for producing plastic parts and products [1, 2]. Complete operation of injection molding requires an injection molding machine with a control unit, a properly clamped mold with a cavity or cavities that define(s) the part geometry, and a mold temperature control unit. The process begins with feeding plastic pellets of about 2 to 3 mm in size into the hopper of the injection molding machine (Figure 1.1). Before feeding, the plastic pellets are dried and cleaned to ensure low moisture content. Additives may be added to the pellets to be fed into the hopper to modify the plastic's or final product's properties.

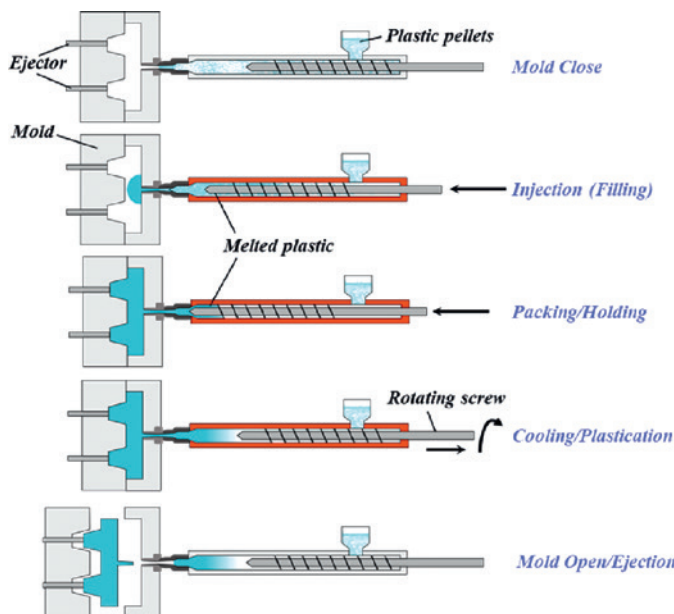


Figure 1.1 Schematic of the injection molding process [3]

The injection screw then rotates and conveys the pellets to the heated barrel of the injection molding machine. The barrel consists of three zones—the feeding zone, the compression zone (transition zone), and the metering zone—all of which may be set to different heating temperatures (Figure 1.2). As the pellets pass through the feeding and compression zones, they gradually melt until they finally become a hot melt within the metering zone. The rotation of the screw provides shear heating resulting from the mechanical crushing of the pellets between the screw flights and the barrel. The shear heating acts as the major heat source for pellet melting. Additional heat is also transferred from the barrel to the pellets via contact, which assists in melting the pellets. The rotation of the screw stops when the proper amount of melt is accumulated from the tip of the screw to the nozzle. The accumulation and conveying of melt within the barrel builds up pressure in front of the screw tip. The pressure pushes back the screw until enough melt for one shot is accumulated. This melt preparation stage is also known as the plasticating stage. In front of the screw tip, there is a shut-off valve to prevent melt entering into the mold during the plasticating stage.

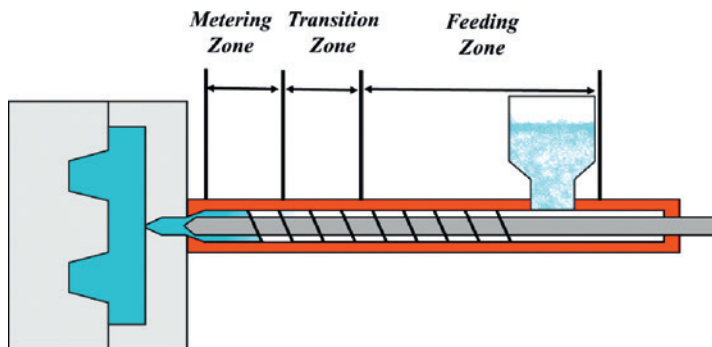


Figure 1.2 Schematic of the three main zones within the injection molding barrel [3]

Once the screw stops rotating, the hydraulic pressure or electrical motor acts to move the screw forward at the profiled speed and push the plastic melt to flow through the nozzle, the sprue, the runner system, and into the cavity. The stage in which the melt begins to flow through the sprue until the cavity is entirely filled is called the mold filling stage. Once the cavity is filled, the screw continues to push additional melt into the cavity under very low speed (pressure-activated) to compensate for the subsequent shrinkage due to melt solidification. The slow advance of the screw under the profiled pressure is called the mold packing/holding stage. The packing stage ends when the gate is completely frozen and no more melt can be pushed into the cavity. The filled melt within the cavity is cooled until the part surface is sufficiently solidified. Then the mold is opened and the part is ejected. This stage of melt solidification is known as the mold cooling stage. The plastic

melt begins to cool as soon as it touches the cold surface of the mold cavity. However, the serious cooling begins when the filling of the cavity ends. The cessation of hot melt flow also indicates that no more heat is being conducted into the cavity. Although cooling continues throughout the entire injection cycle, the cooling stage is usually recognized as the period between the end of the packing stage and the beginning of part ejection.

When the gate is frozen, the screw can begin rotating and plasticating the melt for the next injection cycle. Thus, one injection cycle (Figure 1.3) includes mold closing, mold filling, mold packing, mold cooling, and mold opening. Plastication begins during the mold cooling stage and may last until mold opening or even before the end of mold closing of the next cycle. Plastic shrinks as it cools from the melt temperature to a solid state. The relationship between pressure, temperature, and specific volume (discussed later), as well as the thermal-mechanical history of material elements, determine the volumetric shrinkage of the parts. During the injection molding process, pressure and temperature gradients exist within the melt and the solidified parts, resulting in non-uniform part shrinkage and associated warpage, which are important issues to be resolved and controlled within acceptable limits during the molding process.

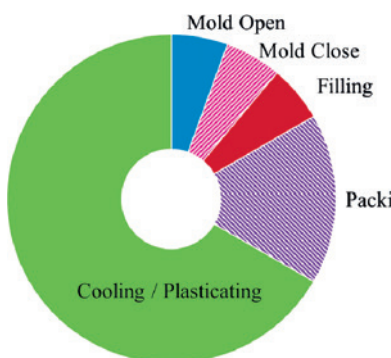
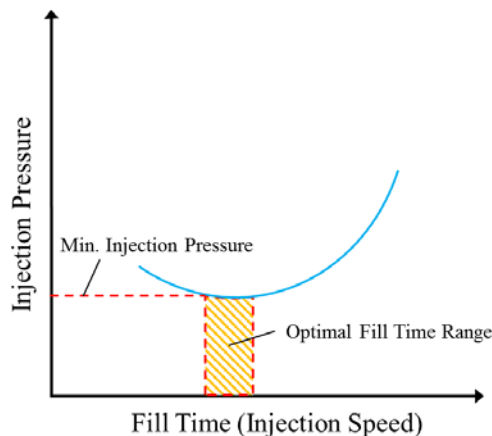


Figure 1.3
Injection molding cycle

1.1.1 Brief Overview of an Injection Molding Machine

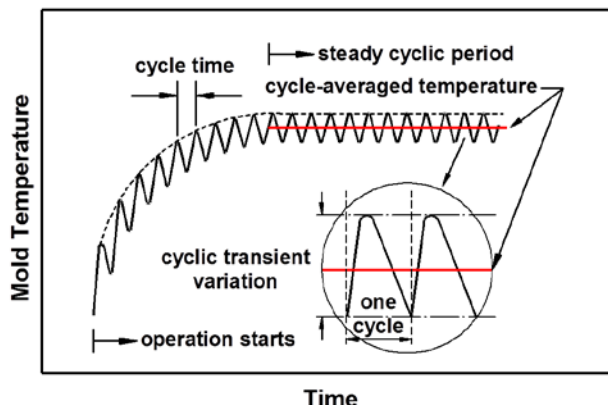
The most popular type of injection molding machine at present is the reciprocating screw injection machine, prototypes of which first appeared in the 1940s and 1950s. The two essential components of an injection molding machine are the injection unit and the clamping unit, whose operation relies on the hydraulic or electrical servomotor system and the associated control system.

**Figure 1.5**

Injection pressure needed for different fill times

1.1.2.4 Mold Temperature

Coolants circulate in the cooling channels to maintain the cavity surface temperature. Cavity surface temperature is determined by coolant temperature, coolant thermal and rheological properties, coolant flow rate, and the corresponding cooling channel dimensions and layout. The mold materials, mold size, and the duration of melt within the cavity, as well as factors such as initial melt temperature, ejection temperature, and part thickness, may also influence the cavity surface temperature. During molding operation, the heat from the hot melt flow should be approximately equal to the heat removed by the coolants. Thus, the coolant flow rate in each branch of the cooling channel should have a high Reynolds number to ensure that the flow is turbulent. Cavity surface temperature is not only intimately related to the cooling time but also significantly affects the part quality. Mold temperature varies in a transient cyclic manner (Figure 1.6) and also varies from location to location within the mold. Thus, the design of cooling channels to achieve uniform cooling and to maintain a relatively constant mold temperature is crucial.

**Figure 1.6**

Mold temperature variation versus injection cycle [5]

An accurate and robust key process variable control system is necessary to ensure the repeatability and reliability of the product quality, and it forms the foundation layer of the overall control and monitoring system. Up to now, most of the research has been focused on the individual process variable control. Recently, some new control strategies were developed that exploit the inherent characteristics of the injection molding process. This chapter reviews the development of control strategies in injection molding applications. The rest of this chapter is constructed as follows: Section 2.2 introduces the traditional feedback control strategies with the adaptive model predictive control as an example, Section 2.3 illustrates the application of a fuzzy inference system in injection molding control, Section 2.4 shows the learning-type control, Section 2.5 introduces a recently developed two-dimensional control algorithm, and Section 2.6 gives the summary and perspectives.

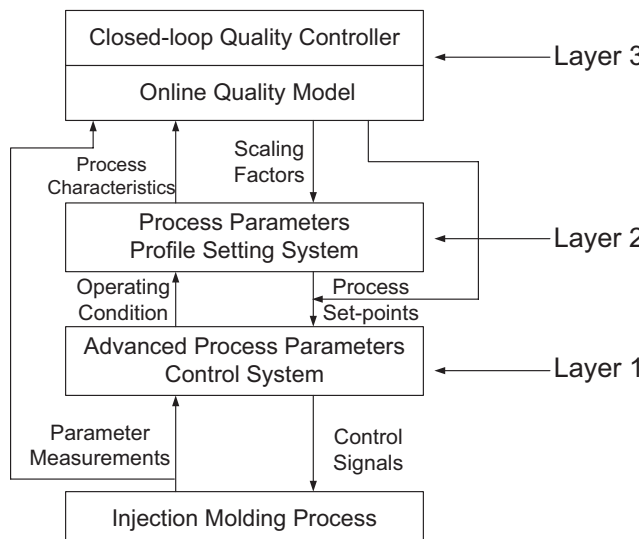


Figure 2.2 Block diagram of a multilayer control system structure

■ 2.2 Feedback Control Algorithms: Adaptive Control

Feedback control is an important class of control algorithms in which the controller receives the signal of the measurement unit and compares it with the desired values to make the control decision. Thus the current control decisions are made based on the observations of the effects of previous decisions. The proportional-integral-derivative (PID) controller is the most widely used feedback control strategy.

It was first developed for automatic ship steering, and it is the most standard feedback control algorithm. It measures the controlled variable, calculates the error between the output and set point, and generates the controller output based on the proportional, the integral, and derivative of the errors. As a simple and general-purpose control algorithm, PID may be the most successful automatic controller in industry. For the injection molding process, PID control is commonly used in the barrel and mold temperature control. In the early practice, it was also used to control some key process variables, such as injection velocity and packing pressure. However, it also has some significant limitations. For example, it only works for linear and time-invariant processes and is not suitable for complex and nonlinear processes like injection molding. Also, the parameters of the PID controller are fixed, so it cannot be used as the core of an advanced control system. The PID control is suitable for continuous processes, since for the continuous process, normally working around a certain operating point, the process dynamics can be linearized in a small range, and PID control can be effective under such circumstances. As a typical batch process, injection molding is stage-based and often operating over a wide range of conditions, so the traditional fixed-parameter controller cannot ensure a satisfactory performance [2].

Due to the batch nature and the nonlinear and time-varying characteristics of the injection molding process, advanced feedback control strategies must be applied to ensure good control performance. Adaptive control is a proper candidate since its parameters are adapted in a certain way to conform to the nonlinear or time-varying process dynamics. There are many different types of adaptive control schemes, such as gain scheduling, model reference adaptive control, dual adaptive control, and self-tuning regulators (STR). The STR, as an important scheme of adaptive control, is used for illustration in this chapter to control some key process variables in injection molding. The basic principle of STR is briefly described in the following sections, and detailed discussions can be found in reference [4].

A self-tuning system is graphically shown in Figure 2.3 [4]. The system is composed of two loops: an ordinary feedback control loop as shown inside the dashed line, and a controller parameter adjusting loop as shown inside the dotted line. The latter, consisting of a parametric model estimator and a controller design calculator, gives an online adjustment of the parameters of the feedback controller. The process model parameters and controller design are updated during each sampling period, with a specified model structure.

There are several methods for process model parameter estimation, for example, least mean squares (LMS), projection algorithm (PA), and stochastic approximation (SA). In this chapter, a recursive least-squares (RLS) estimator is used due to its good sensitivity and superior convergence property [4]. A model predictive control (MPC) design is adopted for the controller design to demonstrate the working procedure of the STR.

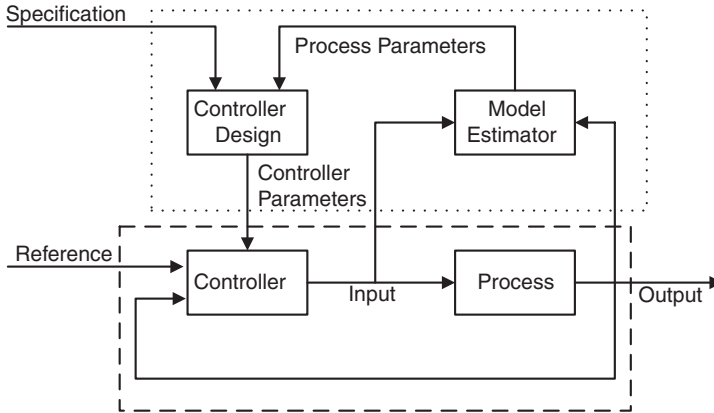


Figure 2.3 Block diagram of an adaptive self-tuning regulator

2.2.1 Model Estimation

Assuming that the process dynamics may be modeled by a discrete time auto-regressive with external input (ARX) model:

$$A(z)y(t) = B(z)u(t - n_d) + e(t) \quad (2.1)$$

$$\text{where } A(z) = 1 + a_1 z^{-1} + \dots + a_{n_a} z^{-n_a}$$

$$B(z) = (b_0 + b_1 z^{-1} + \dots + b_{n_b-1} z^{-n_b+1}) \cdot z^{-n_d}$$

and u are the inputs to the process, y are the corresponding observed process outputs, z is the z -transform (time shift) operator, and n_a , n_b , and n_d are the orders of the A and B polynomials and the process delay, respectively.

We introduce the process model parameter vector

$$\theta^T = [a_1 \dots a_{n_a} \ b_0 \ \dots \ b_{n_b-1}] \quad (2.2)$$

the regression vector

$$\varphi^T(t) = [-y(t-1) \ \dots \ -y(t-n) \ u(t-n_d) \ \dots \ u(t-n_d-m+1)] \quad (2.3)$$

and the loss function

$$V(\theta, t) = \frac{1}{2} \sum_{i=1}^t (y(i) - \varphi^T(i)\theta)^2 \quad (2.4)$$

The model parameter θ , which minimizes $V(\theta, t)$, the differences between the output observation, $y(t)$, and its prediction, $\varphi^T(t)\theta$, in the least-squares sense, is given recursively by

$$\theta(t) = \theta(t-1) + K(t)(y(t) - \varphi(t)^T\theta(t-1)) \quad (2.5)$$

$$K(t) = P(t-1)\varphi(t)(\lambda I + \varphi(t)^T P(t-1)\varphi(t))^{-1} \quad (2.6)$$

$$P(t) = (I - K(t)\varphi^T(t))P(t-1) / \lambda \quad (2.7)$$

Note that λ in Equations (2.6) and (2.7) is a forgetting factor that dictates how fast the model is updated. The value of λ is $0 < \lambda \leq 1$; the smaller λ is, the faster the estimator can track the model changing. A small λ will also make the estimation more sensitive to measurement noise. In this project, λ is set to be 0.98 for injection velocity control and 0.99 for packing pressure control as the selections produce good estimates. As a rule of thumb, the estimate is based on the last N -step results, and N can be calculated as below [4]:

$$N = \frac{2}{1 - \lambda} \quad (2.8)$$

2.2.2 Model Predictive Control (MPC): Generalized Model Control (GPC)

2.2.2.1 Basic Principle of MPC and GPC

Model predictive control (MPC) [5] is a class of advanced process control algorithms. It was originally developed for process industries such as chemical and petrochemical plants in the late 1970s. The research on MPC, both academically and in industrial applications, grew rapidly during the last several decades. The wide application of MPC is mainly due to the following:

1. MPC can be used to deal with complicated process dynamics, including nonlinearity and time-varying characteristics, long time delay, and open-loop instability.
2. MPC can deal with constraints in the process control naturally and systematically.
3. MPC can be extended to multivariable control easily.
4. Feed-forward control is inherently built in to the MPC design, so the process disturbances can be compensated for.
5. MPC is suitable for batch processes since the reference trajectories of the process settings are known before the cycle starts.

6. MPC is a totally open control methodology following certain basic principles for further development and extension.

Due to the above advantages, various MPC algorithms have been proposed: model algorithmic control (MAC), dynamic matrix control (DMC), generalized model predictive control (GPC), and predictive functional control (PFC). These designs all share the same basic features of MPC:

1. Prediction of future outputs based on an internal dynamic model of the process
2. Calculation of an optimal control sequence by minimizing a predefined objective function
3. A receding horizon strategy that moves the control forward toward future sampling times

The basic principle of model predictive control is schematically shown in Figure 2.4, where the prediction, optimization, and receding of the MPC are clearly illustrated.

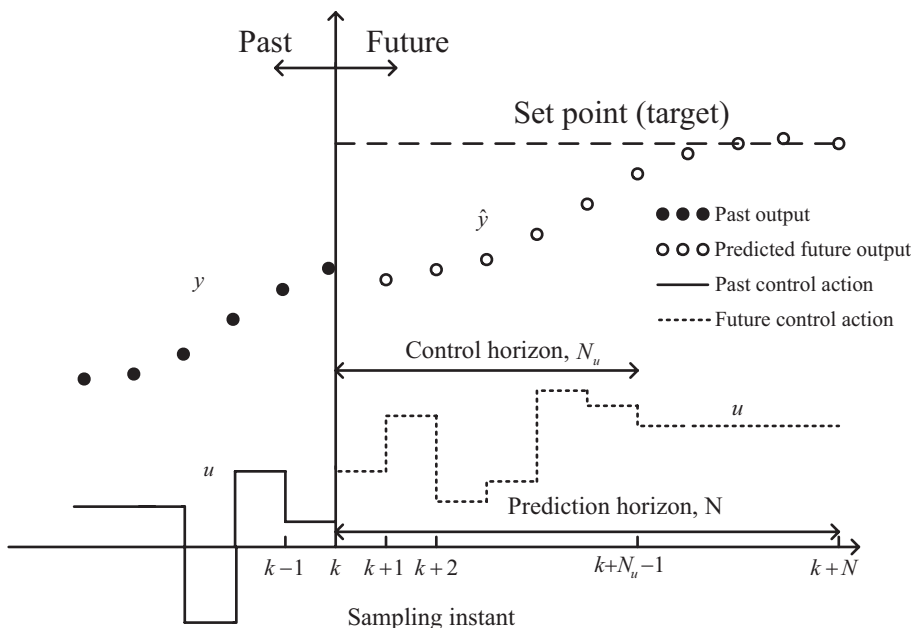


Figure 2.4 Schematics of the model predictive control algorithm

In this chapter, the GPC design is applied to demonstrate the good performance of MPC. The GPC design was first proposed by Clark, Mohtadi, and Tuffs [6]. This control has been shown to be effective with model uncertainty in many process industry applications. To overcome the nonlinear time-varying characteristics of the injection molding process, an adaptive GPC scheme as shown in Figure 2.3 is

2.4.5 P-Type ILC for Packing Pressure

To further demonstrate the performance of iterative learning type control algorithms, the P-type ILC is extended to packing pressure control. Due to the severe time-varying characteristics of the packing pressure dynamics and relatively larger time constant, the sampling rate of the controller is determined to be 50 ms, much longer than that of the injection velocity. The proportional learning rate is selected to be 0.001, also with a series of trial-and-error tests. The designed ILC is applied to experimentally control the packing pressure, and the results are shown in Figure 2.25.

The first cycle's control valve opening is set to be open-loop again, and the pressure response is far from the set-point profile. After five cycles of learning, the sixth cycle's pressure is close to the set point, especially for the first half of the packing. The SSE converging procedure is shown in Figure 2.26. The successful application of packing pressure control again proved the good potential of iterative learning type control algorithms.

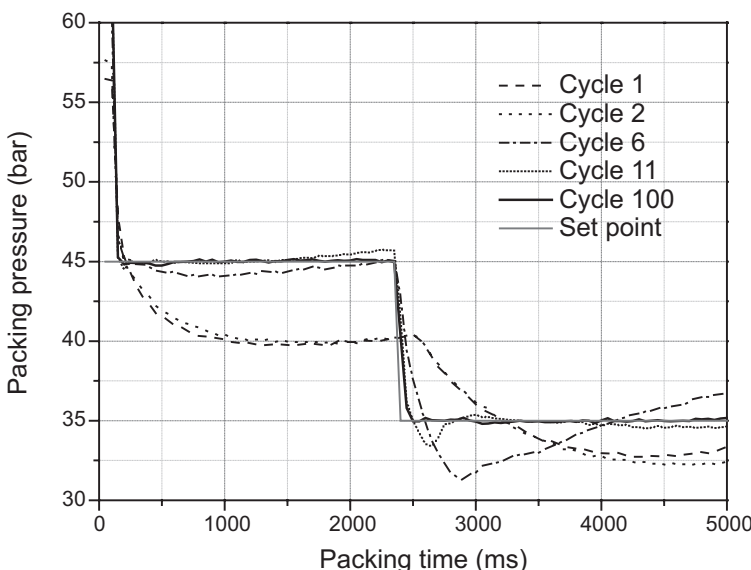


Figure 2.25 Packing pressure P-type ILC result

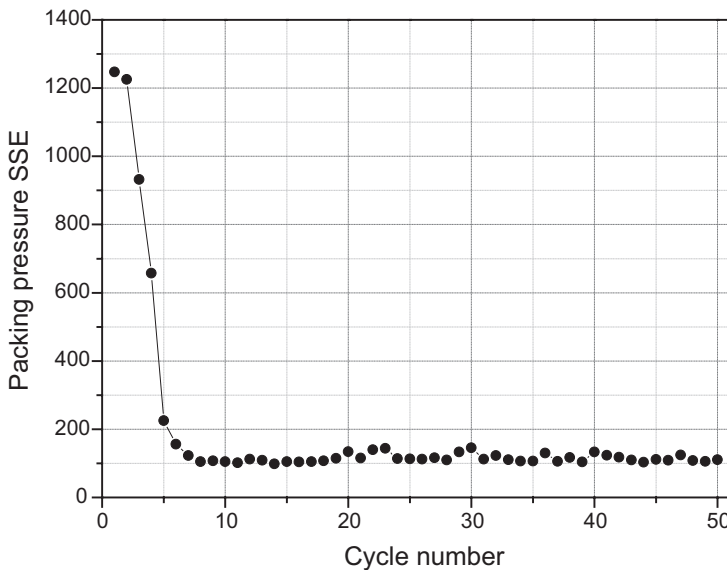


Figure 2.26 SSE converging procedure of the P-type ILC for packing pressure

■ 2.5 Two-Dimensional Control Algorithm

2.5.1 Two-Dimensional Control Background

Injection molding is a typical batch process; it has its own characteristics in comparison to a continuous process. The obvious differences between a continuous process and a batch process like injection molding are (1) a batch process has a finite duration, (2) a batch process repeats itself until the specified amount of products has been made, and (3) a batch process is processed by an ordered set of activities. These characteristics make the control schemes proposed for a continuous process ill-suited for injection molding. Modifications of the original control algorithms have to be made to cope with these features. To summarize the difference between injection molding and traditional continuous processes, the distinctive nature of an injection molding process has three aspects:

- Repetitive nature: the injection molding process repeats itself batch to batch to produce the same products.
- Two-dimensional (in time) dynamics nature: there are within-batch and batch-to-batch dynamics in injection molding simultaneously.
- Multiphase nature: an injection molding process consists of more than one phase.

We found that a water level of ~0.4 wt % decreased the warpage by approximately 0.6 to 0.2 mm and 0.4 to 0.1 mm at cycle times of 31 and 41 seconds for TPO containing 0.5 wt % AC and NC, respectively. Even a water level of 0.24 to 0.26 wt % could decrease the warpage by approximately 0.5 to 0.1 mm and 0.3 to 0.1 mm at the same cycle time for TPO containing 0.5 wt % AC and NC, respectively. The effect of water on warpage reduction was more significant at short cycle times, and AC was more efficient than tubular clay because of its better water-retention capacity. It is clearly seen from both figures that the solid parts could not be demolded at 26 seconds of cycle time without sprue breakage.

5.5.2 Flow Marks and Surface Quality

Similar to microcellular injection molding, flow marks (swirling patterns) were observed on the surface of molded parts in the presence of water. The higher the water content, the more noticeable are the water marks on the surface of the molded part. As discussed in the earlier section, the flow marks are caused by water released as steam at the melt front during filling. Quantitative measurement of the flow marks was done by measuring the surface roughness of the sample. Measurement was done using Veeco Wyco NT9100 laser profilometer. The measurements, using both flat plate and disk specimens of ASTM molded parts, are summarized below.

Flat Plate Mold

Figures 5.19 and 5.20 show the surface roughness of the samples discussed in the previous section, which were molded at different cycle times and at two water levels. The surface roughness of solid TPO with 0.5 wt % NC, which was molded at 41 seconds of cycle time, is included for reference (the last column in the plot). We found that the surface roughness more than doubled as the water content was increased from 0.24 to 0.35 wt %. However, the surface roughness was nearly independent of the cycle time, implying that flow marks were formed mainly during the filling stage.

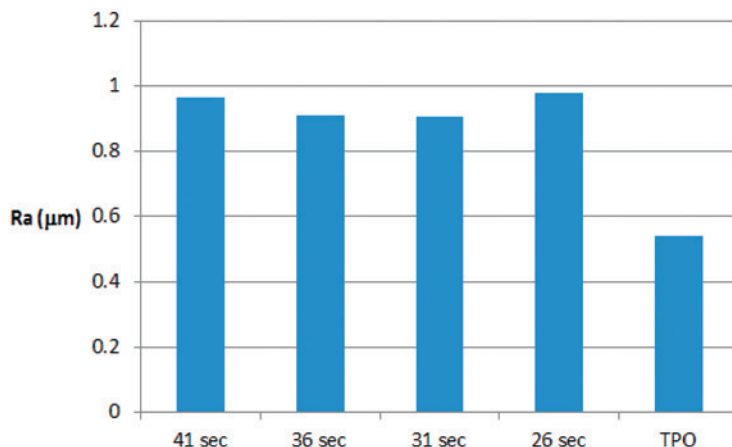


Figure 5.19 Surface roughness of TPO with 0.5 wt % NC and 0.24 wt % water

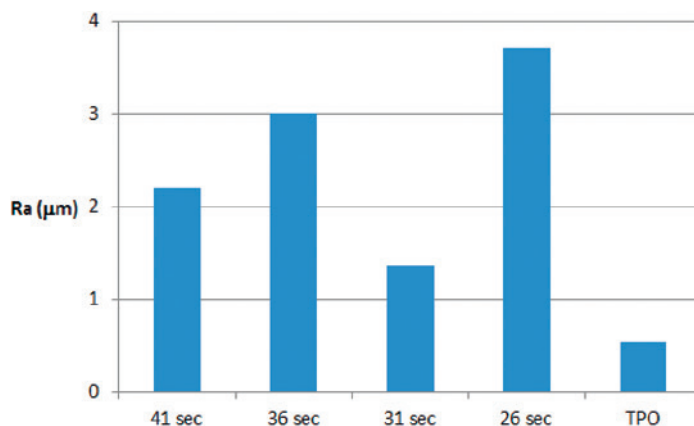


Figure 5.20 Surface roughness of TPO with 0.5 wt % NC and 0.35 wt % water

ASTM Mold

The flow marks on parts molded using the ASTM mold were quantified by measuring the surface quality of the impact disk specimen. In the molding experiment, the melting temperature of the polymer (205 °C and 250 °C) and the injection speed (from 1 to 0.1 second) were varied to investigate their effects on surface roughness (Ra). The initial water content for pressurized TPO with 0.5 wt % AC was 0.42%. The surface roughness of solid TPO parts is also included as a base comparison and summarized in Table 5.8.

Table 5.8 Summary of Surface Roughness Measurements of TPO Molded at Various Conditions

Material and Molding Conditions	Injection Time (s)	TPO 0.5 wt % AC Ra (μm)
Solid, $T_{\text{melt}} = 205^\circ\text{C}$	1	0.51
Press, $T_{\text{melt}} = 205^\circ\text{C}$	1	3.61
	0.25	1.41
Press, $T_{\text{melt}} = 250^\circ\text{C}$	1	1.54
	0.25	1.19
	0.1	1.07

The residual water content of molded parts of pressurized TPO with 0.5 wt % AC was measured to be ~0.2 and 0.1 wt % at melting temperatures of 205 °C and 250 °C, respectively. This indicates that a higher melting temperature would decrease the residual water content, and more water was lost during the molding process. We found that it is very likely that, at higher melt temperature, more water was evaporated inside the barrel during the melting stage, and therefore less water was available in the melt during filling, resulting in a lower value of Ra. We found that the injection time affected the surface roughness since a higher injection speed allowed less time for the steam to escape. In this case, the surface roughness measurements showed a lower Ra as the injection speed was increased.

5.5.3 Hiding the Flow Marks Using In-Mold Coating

A molding trial using pressurized water pellets was carried out at CK Technologies Inc. (Montpelier, OH), which specializes in molding parts for the commercial truck and bus markets. The TPO supplied by CK Technologies was similar to the one previously used and was compounded with 0.5 wt % AC and pressurized to obtain an initial water content of 0.4 wt %. The experiment was done using a Battenfeld injection-molding machine with a flat plate mold with dimensions of 15.3 × 10.87 × 0.32 cm. This mold was equipped with an in-mold coating (IMC) injection port, which was located at the top of the sleeve facing the back platen. The IMC material used was a commercial IMC material provided by OMNOVA Solutions. The IMC coating material was initiated with 0.25% Luperox-26 (*tert*-butyl peroxy-2-ethylhexanoate manufactured by Akzo Nobel Polymer Chemicals LLC for low-temperature applications) and 1.75% TBPB (*tert*-butyl peroxybenzoate manufactured by Arkema Canada Inc. for high-temperature applications). The coating was injected while the part was still in the mold, which was 18 seconds after the packing stage. The curing time for the coating was 72 seconds.

We found that lower packing pressures could be used to obtain a completely filled part using the pressurized pellets. For the solid, the minimum packing pressure needed to obtain a part without a short shot was 3.5 times larger than for the pres-

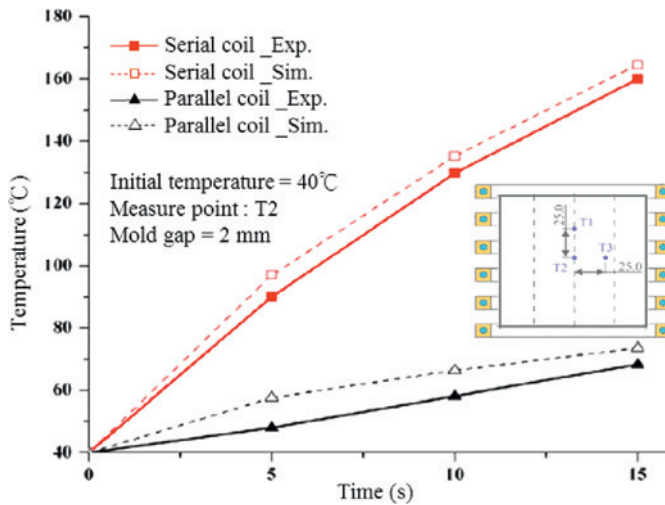


Figure 6.33 Variations of surface temperature at point T2 with regard to time for various coil designs [6]

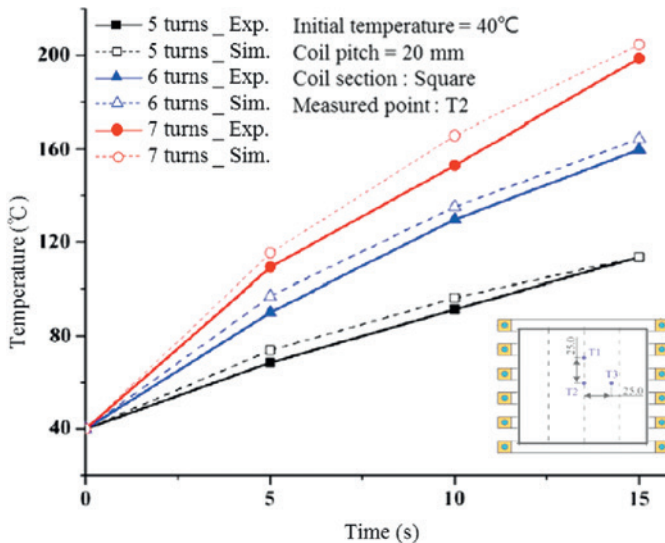


Figure 6.34 Comparison of temperature at point T2 with regard to time given a different number of turns [6]

6.4.7 Induction Heating from the Mold Interior Using Embedded Coils

In the internal coil induction heating (ICIH) method, water cooling is integrated into the injection mold base; hence, the overall heating and cooling effects should be considered together. Figure 6.35 shows schematically the configuration of the

ICIH. When the induction coil is embedded inside the mold, the heat will transfer from the bottom portion of the mold plate to the top surface after heating. One feasible practical configuration is depicted in Figure 6.36.

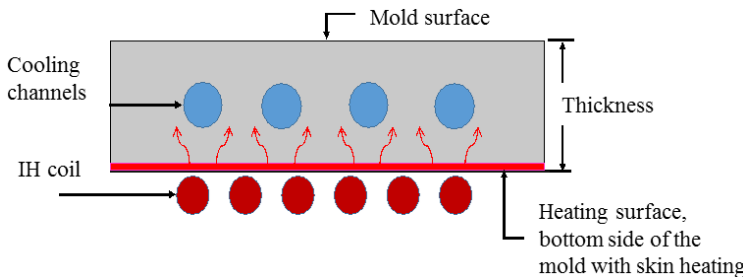


Figure 6.35 Configuration of internal induction heating; the induced heat energy will transfer from the heating surface on the bottom side to the upper cavity surface

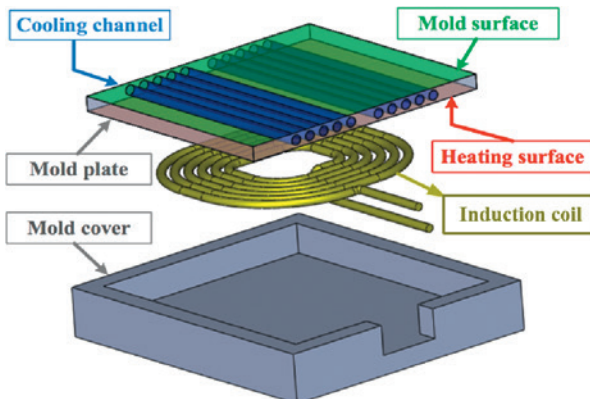


Figure 6.36 Mold structure with embedded internal coil and cooling channels [9]

For internal induction heating, the distance from the induction coil to the cavity surface is one of the most important design parameters. For a top mold plate of 15 mm and 20 mm in thickness, the heating speed was evaluated [32–35] and can be seen in Figure 6.37 under specific operating conditions.

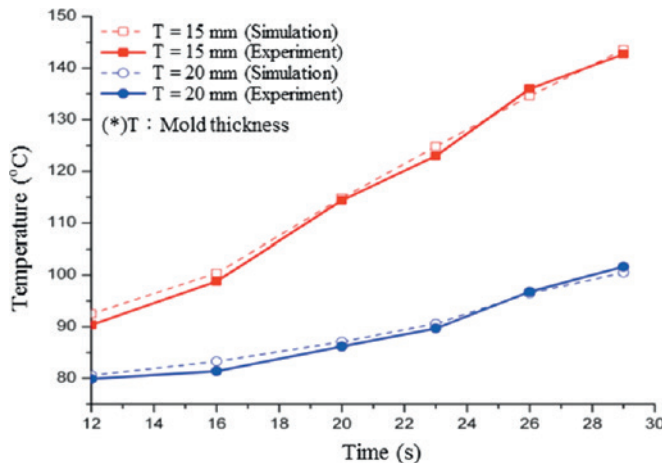


Figure 6.37 Comparison of heating speed results with a mold thicknesses of 15 mm and 20 mm [9]

In the general design of ICIH, if the cooling channels are laid out between the coils and mold surface, control associated with water cooling has a strong influence on the temperature distribution. When the water flows continuously during the heating period, it will lower the heating efficiency and temperature distribution. In contrast, when the water stops running or is drained from the channel, the resulting mold surface temperature will be higher and the temperature distribution will improve as well, as indicated in Figure 6.38.

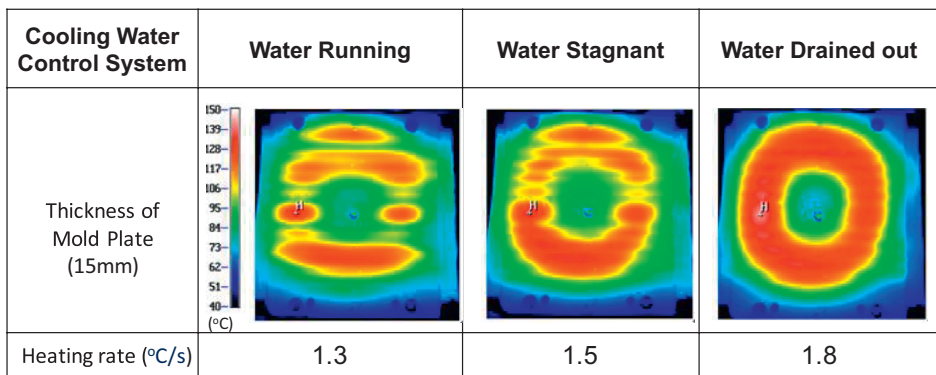


Figure 6.38 Mold plate surface temperature distribution with different methods of water switchover control [32]

For real-world applications of ICIH in the injection molding process, an embedded induction coil is used as the heating source to increase the mold surface temperature. In general, injection molding has three main stages. The mold is first heated

distribution were found for LDPE, although LDPE had a lower melt strength and showed a larger error bar for the cell size experimental data. Simulation results of microcellular injection molding for SCF nitrogen dissolved in PP showed fairly good agreement with experimental data.

■ 7.5 Gas-Assisted Injection Molding

7.5.1 Introduction

The gas-assisted injection molding (GAIM) process utilizes compressed gas as the “packing medium”, hence resulting in a lower injection/packing pressure and clamp tonnage compared to those of the conventional injection molding process. Furthermore, GAIM aids in the molding of thick-walled parts, produces significant weight saving, reduces if not eliminates part warpage and sink marks due to reduced filling pressures and residual stresses, and results in shorter cooling times by coring out the thick portion of the part [25].

However, controlling the processing conditions, such as delay time, gas holding time, injected gas pressure, and the amount of injected melt, are critical to ensure consistent gas penetration in the cavity [26]. The most well-known problem is rigidity degradation for rib-strengthened thin plates where the ribs also serve as gas channels in GAIM. When ribs are hollowed by the injected gas during gas-assisted filling, a large void in the core of each gas-channelled rib is created. Thus, rib rigidity is greatly reduced. This problem has been investigated by many researchers [27, 28]. Obviously, the rib design guidelines for conventional molding cannot be applied directly to GAIM.

The 2.5D generalized Hele-Shaw (GHS) approximation has been extensively adopted to model conventional injection molding as well as the GAIM process [29]. However, the nature of the 3D flow inherent in the gas penetration phase invalidates the 2.5D GHS assumptions. Moreover, the irregular cross-section of the gas channel cannot be accurately modeled through the use of a 1D rod element as in the 2.5D approach. An unreliable estimation of geometry-related flow resistance and heat transfer, and furthermore, the prediction errors for the melt front location and gas penetration length, may occur [30, 31].

The gas-assisted injection molding process is a more complicated process than the conventional injection molding process because of its 3D flow characteristics and the instability of the gas bubble. In this section, based on 3D simulation of injection molding, a combination of FVM and a volume-tracking method were further extended to simulate the melt flow as well as the gas penetration in GAIM.

7.5.2 Governing Equations

In this approach, the fluids are considered to be incompressible and Newtonian for the air and injected gas phase or generalized Newtonian fluid for the polymer melt phase. Surface tension at the fluid front is neglected. A set of governing equations to describe the transient and non-isothermal fluid behaviors for channel flow and mold filling have been described in Equations (7.1) to (7.7) in Section 7.2.2. Here, the volume fractional function f is introduced to track the evolution of the melt front and gas penetration. In particular, $f = 0$ is defined as the air or gas phase and $f = 1$ as the polymer melt phase, where the melt front is located within cells with $0 < f < 1$. In this study, the injected gas and the air are assumed to be the same fluids with identical properties. The advancement of f over time is governed by the following transport equation.

$$\frac{\partial f}{\partial t} + \nabla \cdot (\mathbf{u}f) = 0 \quad (7.28)$$

During the polymer melt filling phase, the velocity and temperature are specified at the mold inlet. While the gas is injected, the gas pressure is specified at the gas inlet. On the mold wall, the no-slip boundary condition is applied, and the fixed mold wall temperature is assumed for the energy equation. For the hyperbolic volume fraction advection equation, only the inlet boundary condition is needed, i.e., $f = 1$ for the polymer injection and $f = 0$ for the gas penetration.

The collocated cell-centered FVM-based 3D numerical approach developed in our previous work was further extended to describe the melt flow and gas penetration in GAIM [5]. The numerical method is basically a SIMPLE-like FVM with improved numerical stability. Moreover, second-order accuracy was carefully maintained during discretization. Pressure, velocity, and temperature were solved in a segregated manner. It is this feature that makes the present approach efficient and robust for solving the thermal flow field in complex three-dimensional geometries.

Furthermore, the volume-tracking method based on a fixed framework was incorporated into the flow solver to track the evolution of the melt-gas and melt-air interfaces during injection. After solving the thermal flow governing equations by FVM, the advancement of the interface at each time step was determined by solving the volume fraction advection equation according to the velocities obtained. The material properties from the updated volume fraction function were calculated, and then the next computation of flow field was initiated. This procedure was repeated until the cavity was completely filled.

7.5.3 Case Study

To realize how gas-assisted injection molding works, both numerical simulation and experimental studies were performed. The model was a spiral tube with a radius of 10 mm [32]. The key dimensions are shown in Figure 7.30. The material was polystyrene (PS, manufactured by Chi-Mei). A 78-ton Battenfeld 750/750 co-injection molding machine was used in this study and the gas injection system was provided by Airmold of Battenfeld with an equipped capability of five-stage pressure profile control. The molding conditions are shown in Table 7.3; the remaining conditions included a mold temperature of 60 °C and a gas injection time of 5 s.

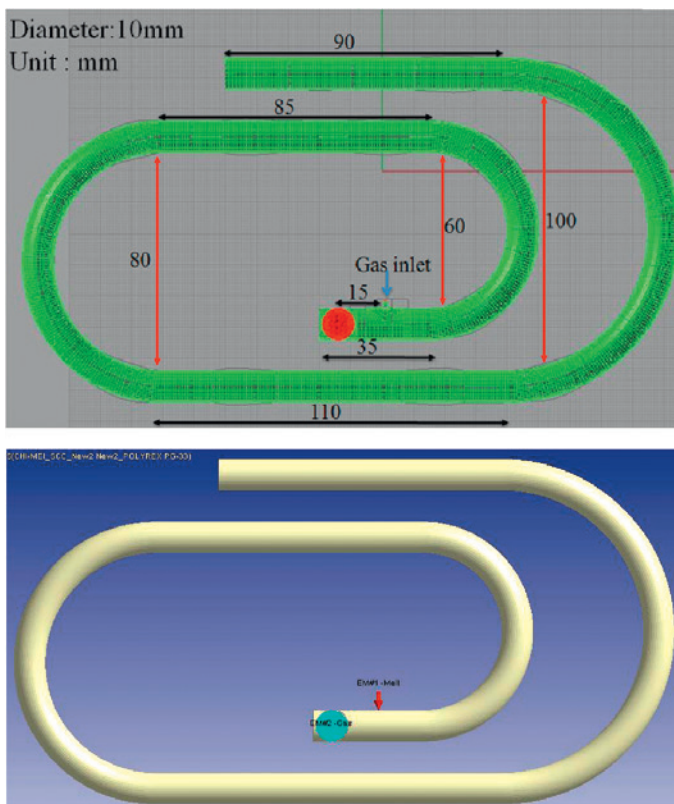
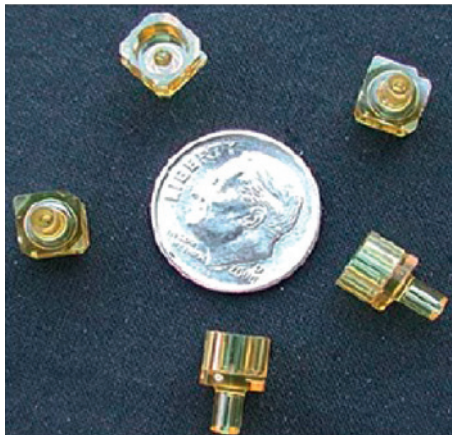


Figure 7.30 Model dimensions and location of gas inlet

In the gas-assisted injection molding process, the melt is hollowed out by gas and forms a skin thickness represented by S as shown in Figure 7.31. The sections of the tube are cut along the gas flow direction and the solidified skin thickness is measured with a caliper. The hollowed-core thickness ratio H equals $(R - S)/R$.

**Figure 9.1**

Microinjection-molded fiber optics housings [1]

■ 9.2 Issues in Molding Parts with Microfeatures

Injection molding of a part with microfeatures, especially microfeatures with high aspect ratios, requires new technological advances and a thorough understanding of the process. Unlike standard injection molding, rapid polymer cooling is amplified in microinjection molding due to the higher ratio of contact surface between the melt and the cold mold wall to part volume. Rapid polymer cooling in microchannels leads to the formation of a frozen layer that stops the melt flow, as shown in Figure 9.2, resulting in incomplete filling or a short shot. Figure 9.3 shows a comparison of typical gap-wise temperature profiles near the end of the fill as the part thickness decreases. For thick sections, the temperature profile through the thickness displays two peaks due to viscous heating. In the case of thin sections, the two temperature peaks vanish, and the increased heat transfer due to conduction results in a decreased average temperature. Further reductions in thickness result in a duplication of the mold temperature across the part thickness, as is the case for ultrathin sections and microstructures. Consequently, a fast melt solidification hinders the melt flow, resulting in a short shot.

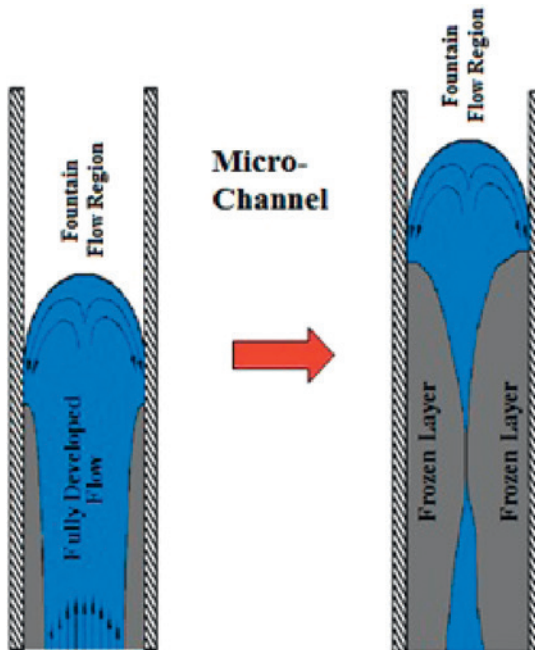


Figure 9.2 Growing frozen layer causes incomplete filling in microchannels

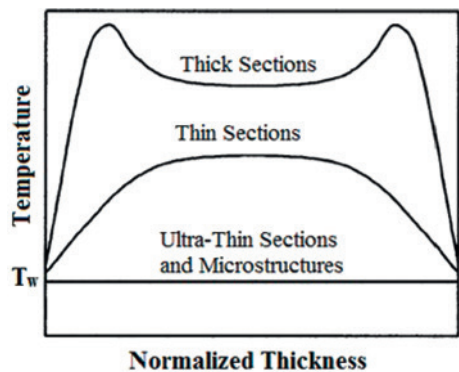


Figure 9.3
Typical gap-wise temperature changes at the end of the fill stage, as part thickness is decreased [2]

In injection molding, the polymer melt freezing time during filling can be predicted from the one-dimensional heat conduction equation:

$$\frac{\partial T}{\partial t} = \frac{k}{\rho C_p} \left(\frac{\partial^2 T}{\partial z^2} \right) \quad (9.1)$$

where ρ is the density, C_p is the specific heat, and k is the thermal conductivity.

Based on Equation (9.1), Equation (9.2) predicts the time for the part center temperature to become equal to the freezing temperature:

$$t_f = \frac{H^2}{\alpha\pi^2} \ln \left(\frac{4(T_p - T_m)}{\pi(T_f - T_m)} \right) \quad (9.2)$$

where t_f is the freezing time, H is the part thickness, α is the thermal diffusivity ($\alpha = k/\rho C_p$), T_p is the initial polymer melt temperature, T_m is the mold temperature, and T_f is the polymer freezing temperature.

Figure 9.4 illustrates a plot of Equation (9.2) for a typical case of $\alpha = 10^{-7} \text{ m}^2/\text{s}$, $T_p - T_m = 100 \text{ }^\circ\text{C}$, and $T_f - T_m = 30 \text{ }^\circ\text{C}$ [3]. The plot shows a linear log-log relationship between part thickness and freezing time. Consequently, as the part thickness decreases, so does the time allowed for the polymer melt to fill the cavity. In the case of ultrathin cavities, the polymer freezes rapidly if a cold mold is used ($< 0.05 \text{ s}$). Although such an effect can be reduced by using a heated mold, the improvement comes at the expense of an increased cycle time due to the increased cooling time.

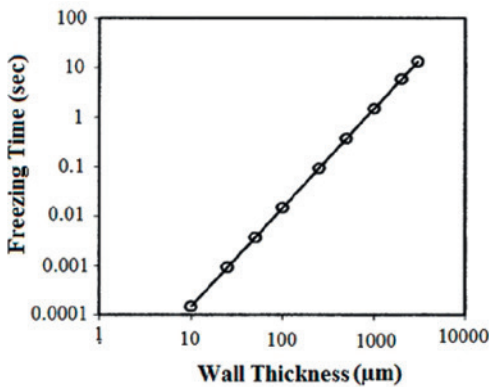


Figure 9.4
Estimated freezing time [3]

In contrast to conventional injection molding, a physical phenomenon called the hesitation effect has to be taken into account when molding microfeatures. To understand the hesitation effect, consider the flow pattern throughout the mold cavity as shown in Figure 9.5. The hesitation effect is common when an injection-molded part contains microfeatures oriented 90° from the main cavity. As shown in the figure, during the injection stage of the melt, filling of the microrib cavity decreases as it moves farther from the gate due to the decrease in injection pressure from the gate to the melt flow front.

The melt that just entered the microrib loses heat until the rest of the mold cavity is filled. When the mold is almost completely filled, the available injection pressure

Index

A

Abbe number 328
aberrations 320

- astigmatism 320, 324, 325
- coma 320, 324, 325
- curvature of field 320, 324, 326
- distortion 320, 324, 327
- longitudinal spherical aberration 324
- spherical aberration 320, 324
- trefoil aberration 320
- wavefront aberration 327, 348

accelerated-aging test 182, 193
acrylonitrile butadiene styrene (ABS) 95, 355
activated carbon (AC) 150, 156
adaptive control 27

- dual adaptive control 28
- gain scheduling 28
- model reference adaptive control 28
- proportional-integral-derivative (PID) 27
- self-tuning regulators (STR) 28

alternating temperature technology.
See pulse cooling
amorphous polymers 364
anisotropy 16
ANSYS FLUENT 111
application layer 394, 398
Arrhenius temperature dependence 239, 332
aspect ratio 216, 354
athermalization 322
autoregressive with external input (ARX) model 29

B

backflow 363
backlight plates 318
back pressure 7
baffle 283
batch foaming 137
batch process 48, 55
biaxial elongation 17
biaxial stretching 123, 137
bi-injection molding 235
bill of materials (BOM) 390
bipolar plates of fuel cells 115
birefringence 19, 301, 305, 306, 308, 309, 311, 313, 319, 320, 329, 332, 333, 335, 346, 347, 348
blow through 94
Boltzmann constant 258
boundary element method (BEM) 332
breakthrough 246
broadband electrical conductivity 116
bubble development model 257

C

CAD/CAM 381
carbon black 118
carbon fibers 118, 127
carbon nanofibers 118
carbon nanotubes 118, 130
cell coalescence 144
cell growth 132, 136
cell morphology 134, 143, 144, 145
cell nucleation 126

charge coupled device (CCD) camera 305
chemical blowing agent (CBA) 121
chemical vapor deposition (CVD) 368
C-MOLD 360
coefficient of thermal expansion (CTE) 322
co-injection molding 235, 238, 245, 249
collaboration 383, 389
compressibility 12
compression molding 235
compression zone (transition zone) 2, 5
computer-aided engineering 318, 331
conductive-filler/polymer composites (CPCs) 115, 116, 146
conductive fillers 118
– carbon black 118
– carbon fibers 118
– carbon nanofibers 118
– carbon nanotubes 118
– graphene 118
– graphite 118
– metallic fibers 118
– metallic nanowires 118
conductivity. *See* electrical conductivity
conductivity anisotropy 133, 134
conformal cooling 235, 313
conformal cooling channel 200, 203
conformal cooling system 281, 283, 287
continuous process 48
convective heat transfer 14, 228
coolant 6, 195
coolant temperature 6, 14
cooling 154
cooling channels 6, 14, 195, 197, 222, 223, 338, 339
cooling time 15
core-pullback 92
core/skin distribution 245
cosmetic defects 23
Cross model 108
– Arrhenius temperature dependence 108
– modified Cross model 108
Cross-WLF model 360

crystallization temperature 364
customization layer 394, 399
cycle time 168, 195, 352
cyclic olefin copolymer (COC) 317
cyclic olefin polymer (COP) 317, 330

D

data layer 394
deflection temperature 15
degree of foaming 136
density 332, 351
density distribution function 250
diamond-like carbon (DLC) 370
differential shrinkage 19
diffusion coefficient 257
diffusion-induced bubble growth 257
dimensionless drag coefficient 252
Dinh–Armstrong hydrodynamic compression force 252
dispersion 121
displacement 339
distribution 121
draft angle 322, 411
dynamic mold temperature control 196, 197

E

eddy current 206, 208, 217
ejection temperature 6, 15, 196
ejector-pin marks 166
electrical conductivity 116, 124, 127, 129, 131, 136, 138, 143
– anisotropic conductivity 120, 126, 129
– in-plane conductivity 120, 133, 134
– through-plane conductivity 120, 121, 129, 134, 147
electric heating 198
electric heating mold (E-mold) 289
electromagnetic induction heating 198, 366
electromagnetic induction technology 206
electromagnetic interference (EMI) 116

electromagnetic interference shielding 115
 electrostatic discharge protection 115
 endothermic nucleation 185
 Euler critical buckling force 252
 external induction heating temperature control (EIHTC) 208

F

fast Fourier transform (FFT) analysis 40
 feedback control 27
 - algorithms 27
 - proportional-integral-derivative (PID) 27
 feeding zone 2, 5
 fiber breakage 120, 122, 127, 129, 132, 136, 141, 146, 249
 fiber interaction 250
 fiber interconnectivity 123, 146
 fiber length 255
 fiber-matrix interaction 250
 fiber orientation 8, 17, 18, 122, 124, 125, 133, 136, 139, 140, 145, 146, 253
 - fiber orientation factors 124
 fiber-reinforced plastic (FRP) 235
 fillers. *See also* conductive fillers
 - carbon fibers 127
 - glass fibers 127
 filling 154
 filling length 356, 357, 362
 filling time 8, 10
 finite volume method (FVM) 271, 301, 313
 flexible capacitors 115
 floating fiber marks 231
 floating marks 195
 flow-induced residual stress 19
 flow-induced stress 12
 flow marks 151, 155, 173, 175
 foam injection molding 115, 119, 124, 146
 - high-pressure foam injection molding 115, 119
 - low-pressure foam injection molding 115, 119

Folgar-Tucker orientation equation 249
 forgetting factor 30
 fountain flow 9, 238, 246, 247
 Fourier number 359
 freezing time 352
 fringe pattern 302, 305, 306, 313
 frozen-in stresses 347
 frozen layer 8
 fuzzy system 37
 - defuzzifier 37
 - fuzzifier 37
 - fuzzy inference engine 37
 - fuzzy inference system (FIS) 38
 - fuzzy rule base 37

G

GAMBIT 111
 gas-assisted injection molding (GAIM) 93, 149, 191, 235, 265, 267, 313
 gas-assisted mold temperature control (GMTC) 227
 gas content 144
 gas penetration 269
 - primary gas penetration 269
 - secondary gas penetration 269
 Gaussian optics 318, 323, 324
 generalized model control (GPC) 30
 generalized Newtonian fluid 238, 266, 272, 331
 glass fiber reinforced composites 103
 - fiber agglomeration 104
 glass fibers 127
 glass transition temperature 157, 196, 334, 355, 364
 graphene 118, 368, 370
 graphite 118

H

halloysite clay 150, 152, 156
 heat transfer coefficient 273, 334, 339, 360, 361
 Hele-Shaw approximation 265, 360
 Hele-Shaw fluid flow model 301

hesitation effect 352, 353
high-density polyethylene 106
high-frequency current (HFC) 224
high-impact polystyrene (HIPS) 94
high-pressure foam injection molding 115, 119
hollowed-core thickness ratio 269, 271
hot gas heating 198
hot runner 235, 271, 273, 313
hydraulic diameter 361
hydrophobic surfaces 370
hysteresis loss 208

I

iARD-RPR model 249, 252
Improved Anisotropic Rotary Diffusion model combined with the Retarding Principal Rate model. See iARD-RPR model
induction coil 209, 210, 222
induction heating 208, 209, 210, 212, 214, 217, 221
induction heating molding (IHM) 289
infrared heating 231
injection-compression molding
- compression force 304
- compression gap 304
- compression speed 304
- compression time 304
- delay time 304
injection-compression molding 235, 301, 313
injection cycle 7
injection molding barrel 2
- compression zone (transition zone) 2
- feeding zone 2
- metering zone 2
injection molding cycle 3, 195
injection pressure 4
injection screw 2
injection speed 4
injection stroke 8
in-mold coating (IMC) 177
insert molding 235, 236

intelligent control 25
internal coil induction heating (ICIH) 220

J

Jeffery's hydrodynamic (HD) model 250
jetting 23
Joule heating 206

K

knowledge management 379, 381, 417
knowledge management navigation system 379

L

laser sintering 281
learning-type control 48
learning-type control methods 49
- iterative learning control (ILC) 49
- repetitive control 49, 50
- run-to-run control (R2R) 49
least mean squares (LMS) 28
lenses 318, 319
light guide plates (LGP) 320
light guides 319
light-path refractive 319
linear expansion coefficients 17
logic layer 394, 396
long-fiber-reinforced plastics 313
long-fiber-reinforced thermoplastic (LFRT) 249
longitudinal spherical aberration 324
low-density polyethylene (LDPE) 259
low-pressure foam injection molding 115, 119
low-thermal-mass mold 365

M

machine control 25
machine scheduling 415
machine variable control 25

machining plan 390
maintenance 383, 391, 395
manufacturing planning 413
material degradation 355
Maxwell equations 207
mechanical properties 170–172, 186, 192, 193
– elongation at break 183, 184
– flexural modulus 188
– modulus 183
– tensile strength 183
mechanism design 411
melt front advancement 8
melt front area 8
melt-pushback 92
melt temperature 4, 5, 15
metallic fibers 118
metallic nanowires 118
metering zone 2, 5
microcellular foam injection molding 184
microcellular injection molding 149, 175, 191, 235, 256, 313
microelectromechanical systems (MEMS) 349
microinjection molding 349, 363, 375
microinjection-molding machine 363
modeling and simulation codes
– ANSYS FLUENT 111
– C-Mold 360
– GAMBIT 111
– Moldex 108
– Moldflow 111, 333, 360
model predictive control (MPC) 28, 30
– dynamic matrix control (DMC) 31
– generalized model predictive control (GPC) 31
– model algorithmic control (MAC) 31
– predictive functional control (PFC) 31
modified Cross model 108, 239, 331, 332
– Arrhenius temperature dependence 108
modulation transfer function (MTF) 320
mold clamping/opening speed 7
mold cooling 14
mold cooling stage 2
Moldex 108
mold filling stage 7
Moldflow 111, 333, 360
mold opening 120
mold packing/holding 12
mold packing/holding stage 2
mold temperature 4, 6, 14
molecular orientation 8, 12, 17, 18, 301
monochromatic aberrations 324
MuCell. *See* microcellular injection molding
multi-component molding 235, 236, 237, 313

N

nanoclay (NC) 156
nanocomposites 95
navigation system 379, 381, 383, 390, 393, 395, 396, 402, 410
non-Newtonian fluid 331
nonslip condition 9
no-slip boundary condition 240, 266
nozzle temperature 5
Nusselt number 361, 362

O

oil heating 199
optical polyesters (O-PET) 317
optimum filling time 5
orientation tensor 250, 253
over-molding 235, 236, 238
– sequential over-molding 240, 242
oxycarbide 370

P

packing 154
packing/holding pressure 4, 13
packing/holding stage 4
packing pressure 13
packing stage 2
packing time 13

penetration depth 206, 207
 percolation curves 130
 percolation graphs 132
 percolation theory 118
 percolation threshold 118, 121, 124, 126, 127, 129, 130, 132, 138, 140, 141, 147
 percolative graphs 130
 phase diagram 153
 photoelasticity 20, 305
 physical blowing agent 119, 144
 pid thermal response (RTR) molding 365
 plasticating stage 2
 plasticizing effect 121
 Plexiglas 317
 PMMA (poly(methyl methacrylate)) 329
 Poisson equation 272, 282, 290
 polyamide-6 95
 - glass fiber reinforced polyamide-6 95
 - polyamide-6/clay nanocomposites 95
 polybutylene terephthalate 95
 - glass fiber filled polybutylene terephthalate 95
 polycarbonate (PC) 106, 272, 290, 317, 329, 366
 - high-density polyethylene (HDPE)/polycarbonate (PC) blend 106
 polyethylene 95, 106
 - high-density polyethylene (HDPE)/polycarbonate (PC) blend 106
 poly(methyl methacrylate) (PMMA) 317
 polypropylene 95, 122, 129, 252, 259, 356, 368
 - glass fiber filled polypropylene 95
 - virgin polypropylene 95
 polystyrene 94, 156, 267, 355
 - general-purpose polystyrene 94
 - high-impact polystyrene 94
 power law index 332
 power law region 332
 Prandtl number 362
 precision injection molding 364
 precision optics 318
 processing conditions 15
 process variable control 25
 projection algorithm (PA) 28

project management 383
 proportional-integral-derivative (PID) control 27
 proportional valve 49
 prototyping 364
 proximity effect 224, 225
 pulse cooling 204
 pvT 16
 - pvT diagram 16
 - pvT model 334
 - pvT path 16

Q

quality control 25

R

radiation heating 198
 rapid heat cycle molding (RHCM) 200, 289
 reciprocating screw injection machine 3
 redevelopment 393, 402, 407, 408, 410
 refraction 321
 refractive index 317, 320, 321, 322, 323, 329, 332, 346
 relative density 136, 138
 residual stress 4, 12, 16, 19, 21, 119, 195, 301, 319, 320, 332, 342, 343, 348, 364
 - external loading on part structure 19
 - flow-induced residual stress 19, 304, 306, 308, 309, 311, 313
 - flow-induced stress 12
 - thermal-induced residual stress 19
 - thermal residual stress 11, 20, 244
 - thermal stress 241, 306, 308, 309, 311, 313
 residual wall thickness 97
 Reynolds number 6, 14, 362

S

scaffolded mold 365
 schedule estimation 390
 Seidel aberrations 320, 324

selective laser sintering 365
 semicrystalline polymers 364
 sequential multiple shot molding 236
 sequential over-molding 240, 242
 servo-valve 48
 shear deformation 17
 shear heating 2, 5, 11, 14, 142
 shear rate 12
 shear stress 12
 shear thinning 355
 shell–core structure 253
 shish–kebab structure 106
 short glass fiber reinforced thermoplastic composites 94
 short shots 331, 364
 shrinkage 3, 10, 16, 17, 19, 191, 301, 332, 354
 shut-off valve 2
 SigmaSoft 334
 silicon carbide 370
 silicone rubber 370
 silicon oxycarbide 370
 sink mark 23, 119, 167, 170, 181, 193, 265, 301
 skin effect 206, 223
 slip-inducing coating 368
 snap-fit 412
 Snell's law 321, 323
 specific heat 272, 332, 351, 365
 specific volume 17
 speed of screw rotation 7
 stainless steel fibers 127
 standardization 383, 386, 395
 steam heating 200
 stochastic approximation (SA) 28
 Strehl ratio 320
 stress optic coefficient 332, 335
 styrene acrylonitrile (SAN) 106
 supercritical fluid molding (SCF molding) 184
 supercritical fluid (SCF) 151, 256
 surface quality 173, 189
 surface reflective 319
 surface roughness 175, 176, 191, 193
 swirling patterns. *See* flow marks

switchover 12
 systematization 383, 395

T
 tangential elongation 17
 thermal conductivity 126, 272, 332, 351
 thermal diffusivity 15, 352
 thermal-elasticity theory 334
 thermal-induced residual stress 19
 thermal management 313
 thermal mass 365
 thermal-mechanical history 16, 17, 20
 thermal residual stress 11, 244
 thermoplastic polyolefin 154, 156
 thin-wall molding 349
 three-dimensional printing 281, 365
 tolerances 321
 total thermal displacement 287
 transition temperature 364
 transmittance 329
 turbulent flow 14
 two-dimensional control 55
 two-dimensional control algorithm 55

U
 ultrathin-wall molding 349
 uniaxial stretching 137
 user-defined function (UDF) 405

V
 variable mold temperature 196
 variable mold temperature control 199
 variotherm 196, 197, 235, 289, 298, 313
 viscosity 332
 void fraction 133, 136, 139–141
 volume exclusion effect 138
 volume fractional function 239, 266
 volumetric shrinkage 17
 V–P (velocity to pressure) switch 373

W

- warpage 3, 16, 19, 21, 173, 186, 189, 190, 191, 193, 237, 241, 242, 265, 287, 301, 306, 308, 309, 311, 313, 319, 321, 331, 332, 338, 339, 354
- water-assisted foaming 149
 - residual water 183
 - residual water content 177
 - water-carrier particles 155, 160, 182, 185, 192
 - water-pressurized pellets 151, 158
- water-assisted injection molding (WAIM) 89, 149, 191, 235
 - blow through 94
 - core-out ratio (CR) 100
 - fingering 99, 100, 103
 - full-shot water-assisted injection molding 90
 - movable-type pin 96
 - overflow cavity 90
 - overflow water-assisted injection-molding 91
 - piercing-type pin 96
 - short-shot water-assisted injection molding 90
 - stationary-type pin 96
 - orifice pin 96
 - porous pin 96
 - ring pin 96

water heating 199, 210

water penetration 97

- core-out ratio (CR) 100

- fingering 99, 100, 103

- primary penetration 97

- secondary penetration 93, 97

water-pressurized pellet injection

- molding. *See* water-assisted foaming

- pressurized water pellets 158

- residual water 183

- residual water content 177

- water-carrier particles 155, 160, 182, 185, 192

wavefront aberrations 327, 348

wavefront image 346, 347

weld lines 23, 195, 331, 364

wire-EDM (electrical discharge machining) 356

Z

Zernike coefficients 346

Zernike polynomials 327

zero shear viscosity 332